UNSYS digital

International Journal of Robotics and Mechatronics

Design and Performance Evaluation of a Self-Controlled Magneto-Rheological Damper

Mohammad Meftahul Ferdaus, M M Rashid, M.M.I. Bhuiyan, and Asan Gani Bin Abdul Muthalif

Department of Mechatronics Engineering, International Islamic University Malaysia, Malaysia

***Abstract*—**Magneto-rheological (MR) dampers are semi-active control devices and use MR fluids. Magneto-rheological dampers have successful applications in mechatronics engineering, civil engineering and numerous areas of engineering. At present, traditional MR damper systems, require an isolated power supply and dynamic sensor, which requires large space. This paper presents the achievability and accuracy of a self-controlled, i.e., self-powered and self-sensing magneto-rheological damper using harvested energy from the vibration and shock environment in which it is deployed. Another important part of this paper is the increased yield stress of the Magneto-rheological Fluids. Magneto-rheological fluids that use replacement of glass beads for Magnetic Particles to surge yield stress is implemented here. Clearly this shows better result on yield stress, viscosity, and settling rate. The permanent magnet generator (PMG) is designed and attached to a MR damper. For evaluating the self-powered MR damper's vibration mitigating capacity, an Engine Mount System using the MR damper is simulated with the help of ANSYS software. The ideal stiffness of the PMG for the Engine Mount System (EMS) is calculated by numerical study. The vibration mitigating performance of the EMS employing the self-powered & self-sensing MR damper is theoretically calculated and evaluated in the frequency domain.

***Keywords*—**Self-powered, MR damper, finite element, self -controlled.

I. Introduction

MAGNETO-RHEOLOGICAL (MR) fluids is a sort of smart material. By changing external magnetic field strength the rheological properties of MR fluids can be varied. Such fluids consist of micron-sized particles, made of magnetic material, suspended in a carrier fluid, normally a type of oil. In the absence of an applied field, the MR fluids exhibit Newtonian-like behavior. However, in the presence of an applied magnetic field, the iron particles acquire a dipole moment aligned with the external field which causes the particles to form linear chains parallel to the field [1]. Magneto-rheological (MR) fluid -based damper is one of the most promising class of semi-active shock absorbers, has been widely applied to control and minimize undesirable vibration and shock for numerous systems such as different types of vehicle suspension systems [4], and civil structures [5] etc. MR dampers possess many performance advantages, including continuously controllable force, quick response, and low power consumption, etc. MR dampers can be analyzed using available models and are amenable to innovative design concepts such as increasing the viscosity of the MR fluids by changing the properties of the fluid. To practically construct vibration and shock mitigation systems using MR dampers, either a power supply or a current amplifier is required to activate the electromagnetic coils in the MR dampers to supply magnetic field to the MR fluid. However, if mechanical energy resulting from vibration and shock can be converted into electrical energy in order to provide power to the MR dampers, then there is a substantial reduction in system volume, weight, and cost that can be realized. MR dampers are typically composed of a piston rod, a piston head, as well as hydraulic and pneumatic reservoirs separated by a floating piston or diaphragm. Inside the hydraulic cylinder, the piston rod is attached to the piston head, which contains the magnetic circuit [7]. When the piston rod assembly moves, the fluid flows through an annular gap in the piston head. Current supplied to the coil in the piston head creates a magnetic field in the gap and increases the yield stress of the MR fluid in the annular gap. This increase in yield stress changes the velocity profile of the MR fluid in the gap and raises the pressure drop down the length of the piston head. In this way, MR dampers can produce controllable field-dependent yield force, in addition to passive velocity-dependent viscous damping force.

This study focuses on the development of a self-powered and self-sensing MR damper operated using the energy harvested from its operating environment, and sedimentation improved new MR fluid's impact on this damper [8]. Also finite element analysis has been accomplished by using ANSYS software version 14.5. For using the new fluid the off state viscosity has increased by 22% and the sedimentation rate decreased slightly [11]. To explain the self-power generation idea, an energy harvesting device that is a permanent magnet generator is considered and added to a MR damper. The generator comprises of a stator, a permanent magnet, and a spring and operates as an energy garnering dynamic vibration absorber of which resonance frequency is matched with a target system whose vibration is to be suppressed. In addition, the resonance frequency of the target system is typically chosen to be much less than the disturbance spectrum in order to take advantage of

Corresponding authors: M.M. Rashid (e-mail: bmahbub@iium.edu.my); Meftahul Ferdaus (e-mail: meftahul.ferdaus@live.iium.edu.my); Asan Gani Bin Abdul Muthalif (e-mail: asan@iium.edu.my)

This paper was submitted on January 17, 2014; revised on April 23, 2014; and accepted on October 27, 2014.

the mount's low transmissibility at high frequency. Generally speaking, vibration isolation systems require high damping near resonance and lower damping above resonance in order to achieve good vibration isolation performance. Therefore, when MR dampers are used for vibration isolation purposes, it would be ideal if the MR damper force can be maximized near resonance and minimized above resonance (see **Figure 3**). If the energy-harvesting dynamic vibration absorber is itself a single-degree-of-freedom (SDOF) system whose natural frequency is matched to that of the target system, then the displacement of the permanent magnet will be greater near the resonance of the target system. Above resonance, the displacement of the permanent magnet is substantially reduced. Thus, for a given dynamic vibration absorber vibration level, the current produced is injected into the magnetic circuit, thereby commanding a damping level proportional to the current produced by the dynamic vibration absorber. Thus, the energy-harvesting dynamic vibration absorber acts as a semi-active control algorithm that produces high current and commands high damping near resonance of the target system, while producing low current and command lower damping above resonance. A key benefit of this approach is that the MR damper no longer needs a sensor to measure motion as a feedback signal to a microprocessor that calculates a control input based on modern control algorithms.

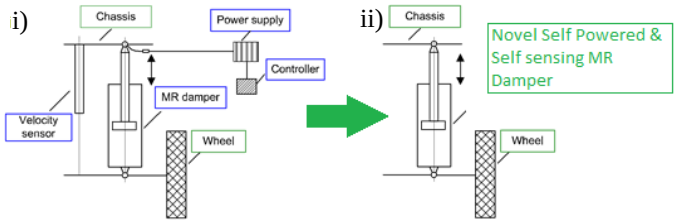

Figure 1 i) Conventional MR damper system ii) Self-controlled MR damper [11]

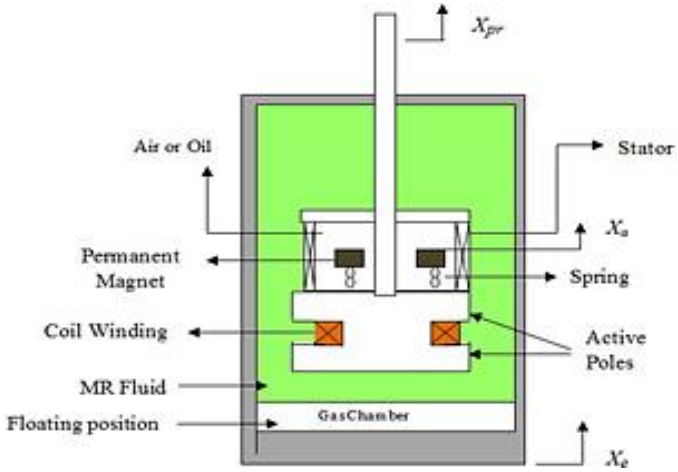

Figure 2 Schematic diagram of proposed self-controlled MR damper [11]

Many researchers such as Russell et al., Nehl et al., Wang and his associates, Or et al., Jung and his associates, Choi and Wereley, Jung et al., Bogdan works on self-powered magneto-rheological dampers [12]. While the previous studies on Magneto-Rheological dampers with self-sensing or power generation functions have presented some favorable results, but this is an integration of the sensing and power generation ability within the same device. Also many researchers has done finite element analysis on conventional MR damper [13]-[15], but here the finite element analysis has been accomplished for verifying the achievability of the proposed self-powered and sensing MR damper model.

II. Self-Powered & Self-Sensing MR Damper

Figure 2 presents a schematic diagram of a self-powered and Self Sensing MR damper.

The hydraulic cylinder contains the piston rod which is attached to the piston head. At one side of the piston head, the PMG is configured. The motion of the permanent magnet as a result of the piston rod motion generates electromotive force *emf* in the stator and the strength of the *emf* is proportional to the velocity of the permanent magnet. So velocity information can be easily calculated from here. The *emf*-induced voltage or current is directly provided to activate the coil winding in the piston head so as to produce a magnetic field into the MR fluid inside the MR valve of the self-powered MR damper.

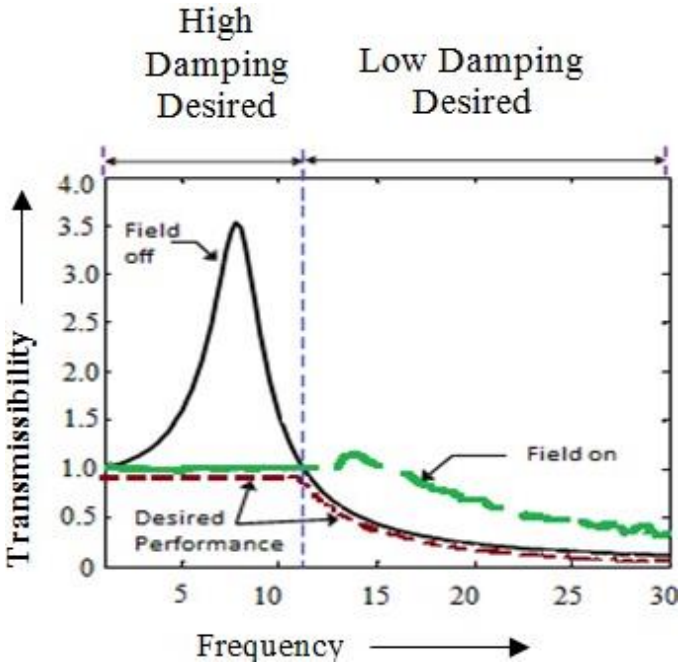

Figure 3 Typical characteristics of vibration controlling system (SDOF) using novel MR damper

Electromotive Force, emf generated by the motion of the permanent magnet in the PMG is given by (1).

$$E_{\text{emf}} = -N_{\text{m}} \frac{d\phi}{dt} = -N_{\text{m}} \alpha B_{\text{m}} \cdot 2\pi r_{\text{m}} \left(\dot{x}_{\text{pr}} - \dot{x}_{\text{pm}} \right) \quad (1)$$

Equation (1) is evaluated with respect to body frame which moves with respect Here, N_{m} is the turn number of the coil in

the stator affected by the permanent magnet at a time, ϕ is the magnetic flux, B_{m} is the magnetic density of the permanent magnet, r_{m} is the radius of the permanent magnet, $\dot{x}_{\mathrm{pr}}$ is the velocity of the piston rod, $\dot{x}_{\mathrm{pm}}$ is the velocity of the permanent magnet, and α is the empirical correction factor for the effective magnetic density of the permanent magnet since there is an air gap clearance between the permanent magnet and the stator. In this study, the design parameters were chosen to be $N_{\mathrm{m}} = 120$ turns, $\alpha = 0.75$, $B_{\mathrm{m}} = 1.3$ T, and $r_{\mathrm{m}} = 15$ mm.

If the time constant, equal to inductances/resistances, of the coils is assumed to be small, the current I produced by the energy harvesting PMG is given by (2).

$$I = \frac{E_{\mathrm{emf}}}{R_{\mathrm{st}} + R_{\mathrm{cl}}} \tag{2}$$

Here, R_{st} is the resistance of the stator and R_{cl} is the resistance of the coil winding. In this study, $R_{\mathrm{st}} + R_{\mathrm{cl}} = 3$ ohm. The force of the self-powered MR damper is given by (3).

$$F_{n\mathrm{MR}} = F_{\mathrm{passive}} + F_{\mathrm{semi}} + F_{\mathrm{gas}} \tag{3}$$

where

$$F_{\mathrm{passive}} = A_{\mathrm{p}}^2 \left(\frac{6\eta L}{\pi r d^3} + \frac{6\eta L_{\mathrm{c}}}{\pi r_{\mathrm{c}} d_{\mathrm{c}}^3} + \frac{6\eta L_{\mathrm{s}}}{\pi r_{\mathrm{s}} d_{\mathrm{s}}^3} \right) \left(\dot{x}_{\mathrm{pr}} - \dot{x}_{\mathrm{e}} \right) + \left(\frac{2\eta\pi r L}{d} + \frac{2\eta\pi r_{\mathrm{c}} L_{\mathrm{c}}}{d_{\mathrm{c}}} + \frac{2\eta\pi r_{\mathrm{s}} L_{\mathrm{s}}}{d_{\mathrm{s}}} \right) \left(\dot{x}_{\mathrm{pr}} - \dot{x}_{\mathrm{e}} \right) \tag{4}$$

where

$$F_{\mathrm{semi}} = \left(2A_{\mathrm{p}} \frac{L}{d} + 2\pi r L \right) \tau_{y_{(H)}} \operatorname{sign}\left(\dot{x}_{\mathrm{pr}} - \dot{x}_{\mathrm{e}} \right) \tag{5}$$

$$F_{\mathrm{gas}} = K_{\mathrm{gas}} (x_{\mathrm{s}} - x_{\mathrm{e}}) \tag{6}$$

Here, A_{p} is the effective piston area, A_{r} is the piston rod area, and x_{e} is the displacement of the hydraulic cylinder. d, d_{c}, and d_{s} are the gaps of the active pole, the coil winding, and the stator, respectively. In addition, r, r_{c}, and r_{s} are the radii of the active pole, the coil winding, and the stator, respectively. The dimensions of L, L_{c}, and L_{s} are the lengths of the active pole, the coil winding, and the stator, respectively. η is the fluid viscosity and $\tau_{y_{(H)}}$ is the yield shear stress of the MR fluid and is assumed to be a function of the magnetic field strength H as follows :

$$\tau_{y_{(H)}} = 1.93 H^{1.73} \text{ Pa} \tag{7}$$

where

$$H = \left| \frac{N_{\mathrm{c}} I}{2d} \right| \tag{8}$$

Here, N_{c} is the turn number of the coil winding in the piston head and K_{gas} is the stiffness due to the gas pressure in the gas chamber and is given by (9).

$$K_{\mathrm{gas}} = \frac{n A_r^2 P_0}{V_0} \tag{9}$$

Here, V_0 and P_0 are the initial volume and pressure of the gas chamber, respectively and n is the specific heat ratio of the gas. In this study, the design parameters were chosen to be $A_{\mathrm{p}} = 1700$ mm^2, $A_{\mathrm{r}} = 79$ mm^2, $L = 20$ mm, $L_{\mathrm{c}} = 15$ mm, $L_{\mathrm{s}} = 30$ mm, $r = 24$ mm, $r_{\mathrm{c}} = 21$ mm, $r_{\mathrm{s}} = 21$ mm, $d = 1$ mm, $d_{\mathrm{c}} = 4$ mm, $d_s = 4$ mm, $\tau_y = 0.18$ Pa·s, and $N_{\mathrm{c}} = 150$ turns.

To emulate a practical force response of the self-powered MR damper, we consider the time response of the semi-active damper force F_{semi} as follows:

$$F_{\mathrm{semi}}^* = \frac{F_{\mathrm{semi}}^* + F_{\mathrm{semi}}}{\tau} \tag{10}$$

Here, F_{semi}^* is the emulated semi-active damper force and τ is the time constant of the self-powered MR damper. In this study, the time constant was chosen to be $\tau = 5$ ms. During a computer simulation, the semi-active damper force F_{semi} will be replaced by the emulated semi-active damper force F_{semi}^*.

III. Finite Element Analysis of The Self-Controlled Damper

The finite element analysis of the proposed self sensing and self powered MR Damper is accomplished with the help of ANSYS software Version 14.5. A 2-D axisymmetric model of the damper is built for analyzing the magnetic circuit.

Error! Reference source not found. shows the area distribution the 2-D axisymmetric model of the self-controlled MR damper. The upper portion is the Power generation part consists of spring, Permanent magnet surrounded by air. The inner piston and outer piston is made of same material that's why both of them are indicated by red color.

Error! Reference source not found. shows the magnetic flux density (B) produced by the coil in accordance to the supplied current generated by the permanent magnet power generated. The variation of the flux color is due to the variation of the magnetic field strength. Red color is indicating the highest strength.

Figure 6 represents magnetic flux density for 2-D and 3-D axisymmetric model. This flux density changes according to the road condition. When vibration is more, movement of the permanent magnet is more. So more current is supplied to the coil and flux density increases. When vibration is less then less flux produced, then magnetic field strength through the fluid is weak as shown in **Figure 6(a)** and **Figure 6(c).** When the vibration is severe then the flux density is high through MR fluid as shown in **Figure 6(b)** and **Figure 6(d).**

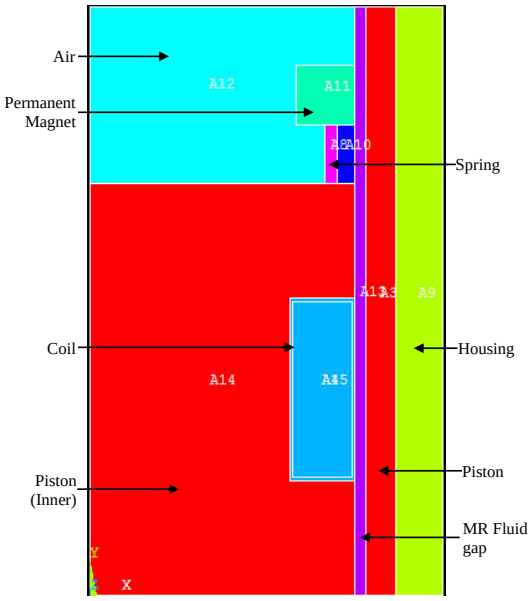

Figure 4 Area distribution of the proposed MR damper in ANSYS

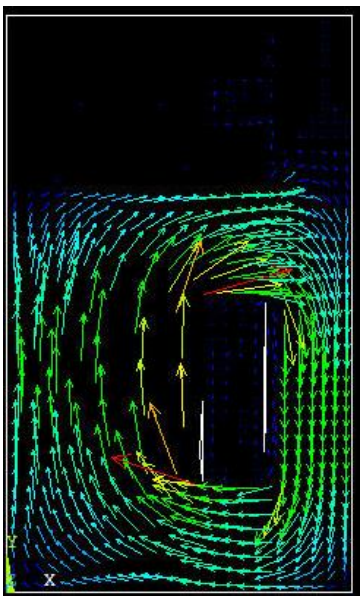

Figure 5 Magnetic flux density

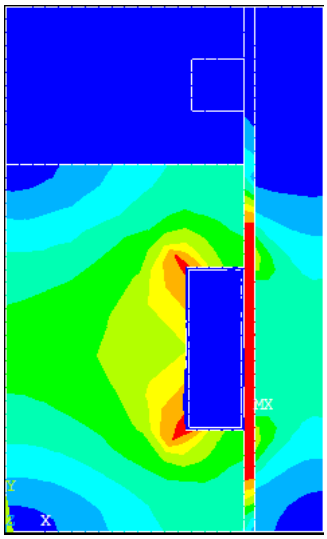

(a)

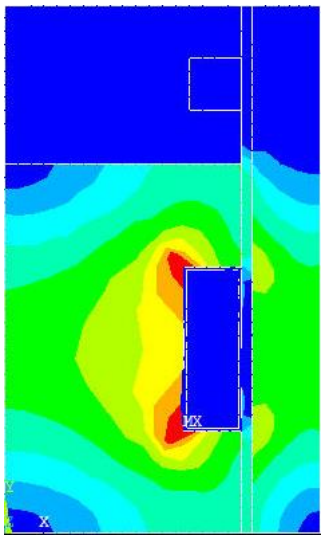

(b)

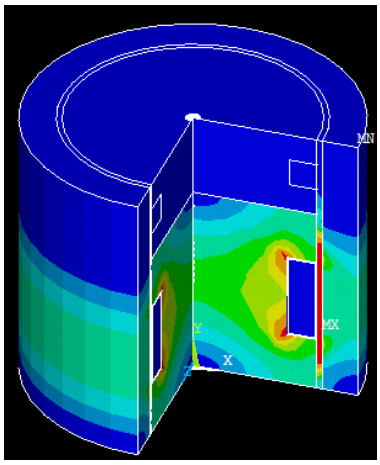

(c)

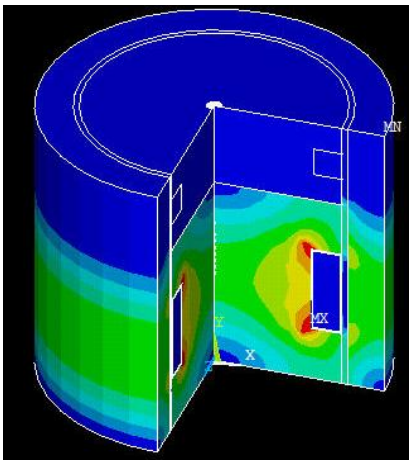

(d)

Figure 6 (a)-(b): Magnetic flux density vector sum before and after magnetic saturation in 2-D; (c)-(d): 3-D axisymmetric model

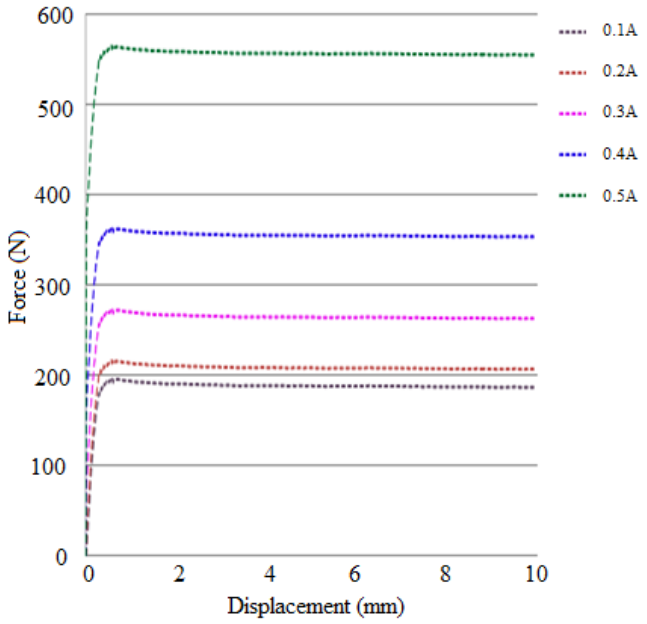

Figure 7 Force vs. displacement curve for different current from ANSYS simulation result

From **Figure 7**, it is clear that as current increasing, the force is increasing. This input current depends on the road condition. When the road surface is rougher, the movement velocity of the permanent magnet is more. So more flux induces as a result more current produced. When more current is supplied to the Damper's coil, more flux is passing through the MR fluid, so the fluid is producing more resistive force.

IV. EMS WITH NEW PROPOSED MR DAMPER

The self-powered & self-sensing MR damper's vibration controlling performance can be theoretically evaluated by considering an EMS (SDOF) with the MR damper as shown in **Figure 8**.

The governing equation of motion for the EMS attach with the new proposed MR damper is as follows:

$$M_s \ddot{X}_{pr} = -(K_s - K_{gas})(x_{pr} - x_e) - F_{passive} - F^*_{semi} + K_a(x_{pm} - x_{pr}) + C_a(\dot{x}_{pm} - \dot{x}_{pr}) \quad (11)$$

$$M_a \ddot{X}_{pm} = -K_a(x_{pm} - x_{pr}) - C_a(\dot{x}_{pm} - \dot{x}_{pr}) \quad (12)$$

Here, M_s is the engine mass, M_a is the mass of the permanent magnet in the energy-harvesting PMG, K_s is the stiffness of the coil spring, K_a and C_a are the stiffness and the damping of the spring in the energy-harvesting PMG, respectively, x is the displacement of the engine mass, and X is the excitation displacement. In this study, representative parameters were chosen to be $M_s = 60$ kg, $M_a = 0.4$ kg, $K_s + K_{gas} = 150$ kN/m, and $C_a = 4$ N·s/m.

Because the resonance of the EMS is 8.0 Hz, an initial choice for the stiffness of the permanent magnet generator was chosen to be $K_a = 1000$ N/m so as to match the resonance of the permanent magnet generator with that of the EMS. However, in order to find an optimal stiffness, we plot the maximum peak value of the transmissibility $|x_{pr}/x_e|$ of the EMS versus the stiffness of the PMG in the self-powered MR damper in Figure 8. From this plot, it was determined that the optimal stiffness value of the permanent magnet generator for the EMS was $K_a = 700$ N/m. This optimal stiffness, $K_a = 700$ N/m, suggests that the resonance of the permanent magnet generator should be slightly below that of the EMS. In this study, the optimal stiffness, $K_a = 700$ N/m, of the PMG for the EMS is used to estimate the vibration controlling capability of the self-sensing & powered MR damper.

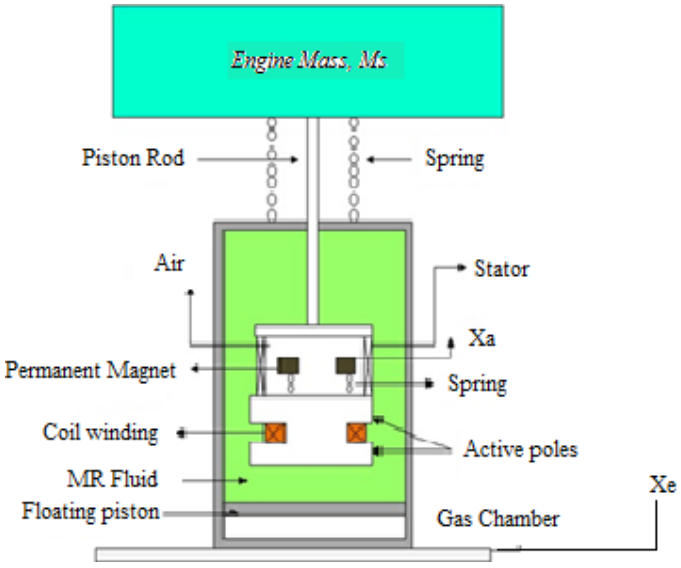

Figure 8 An EMS attached with the self-controlled MR damper

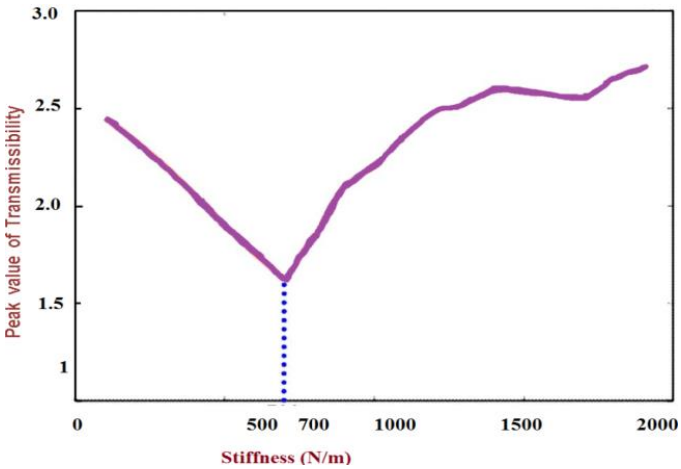

Figure 9 Maximum peak value of the transmissibility of the EMS versus the stiffness of the permanent magnet generator [9]

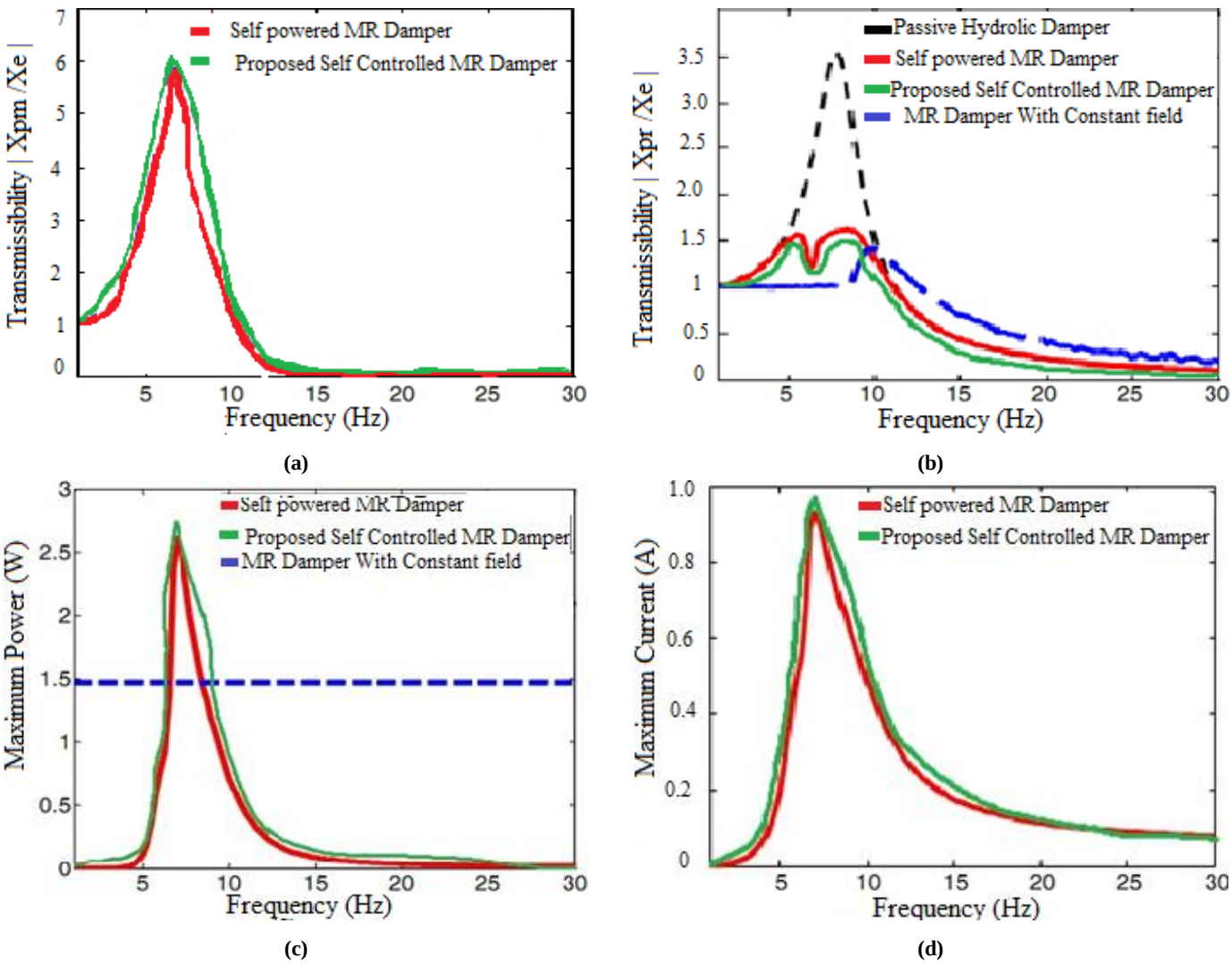

Figure 10 Simulated transmissibility of the vibration controlling system with the self-powered & sensing MR damper filled by MRF-40 & New MRF-37, where (a) Transmissibility of the engine mass x_{pr}/x_e, (b) Transmissibility of the energy-harvesting DVA X_{pm}/X_e, (c) Maximum current, and (d) Maximum power [10]

V. Performance Evaluation

Error! Reference source not found. presents the simulated transmissibility of the EMS with the self-powered MR damper. In this case, a sinusoidal excitation displacement with constant amplitude of 1.0 mm was used. Note that the key benefit of the semi-active control system is to reduce the effects of resonance in the engine mass without increasing high frequency transmissibility. In **Figure 10**, the dash-dotted line represents the passive hydraulic damper that has the same geometric dimension as the self-powered MR damper without the energy-harvesting PMG, the dashed line represents the MR damper with constant field that has a MR valve in the piston head and is applied at the current of 0.7 A from an external power source, and the red solid line represents the self-powered MR damper and green solid line represents self-powered & self-sensing MR damper with new fluid. In Error! Reference source not found.**(a)**, the MR damper with constant field can mitigate resonance, but increases transmissibility above resonance. The self-powered MR damper also substantially reduces transmissibility of the target system at resonance, but it does not increase transmissibility above the crossover frequency. This results from the fact that the energy-harvesting PMG produces a current proportional to the motion of the target system mass, as shown in **Figure 10(b)** and **Figure 10(c)**. The maximum power of the self-powered MR damper is 2.6 W (**Figure 10(d)**), and the power consumption of the MR damper with the constant current of 0.7 A is 1.5 W. Overall, the self-powered MR damper shows good vibration isolation performance over the simulated excitation frequency, and self-powered & self-sensing MR damper with new MRF shows much better vibration controlling performance with more control ability.

VI. Concluding Remarks

In this study, the achievability and accuracy of a self-powered & sensing MR damper that operates using energy

harvested from the operating environment were addressed. A PMG was theoretically constructed and added to a MR damper and also experimented with two new MRF with a little mixing nonmagnetic particle. The dynamic equation for the self-powered & self-sensing MR damper was derived theoretically. In order to theoretically evaluate the vibration controlling capability of the self-powered & self-sensing MR damper, a SDOF EMS using the MR damper was constructed and its governing equation of motion was theoretically derived. In order to find the optimal stiffness of the PMG, a parametric study was conducted. This parametric study indicated that the optimal stiffness was slightly lower than the stiffness required matching the PMG and engine mount frequencies. The isolation performance of the EMS with the self-powered MR damper was calculated in the frequency domain. It was observed through this theoretical analysis that the self-powered MR damper can provide good vibration isolation performance using neither a sensor nor a control processor/algorithm. And on the other side, replacing the ordinary MRF with new MRF with glass beads presented a significant enhancement in yield force, off-state viscosity, etc. With this power generation and self-sensing features, this new MR damper could bring great benefits for the MR damper systems such as saving energy, size and weight reduction, lower expenses, and less preservation. Also finite element analysis has been accomplished for better understanding the achievability of the proposed damper model.

ACKNOWLEDGMENT

The author would like to acknowledge C.H. Chen and W.H. Liao for their explanation of self-sensing and self-powered MR Damper, and also like to thanks Department of Mechatronics, International Islamic University Malaysia for giving the opportunity of using Smart Material and Vibration control Lab.

REFERENCES

[1] W.I. Kordonsky, “Magnetorheological effect as a base of new devices and technologies”, Journal of Magnetism and Magnetic Materials, vol. 122, no. 1, pp. 395-398, 1993. CrossRef

[2] O. Ashour, C.A. Rogers, W.I. Kordonsky, “Magnetorheological fluids: materials, characterization, and devices”, Journal of Intelligent Material Systems and Structures vol. 7, no. 2, pp. 123-130, 1996. CrossRef

[3] L. Zipser, L. Richter, U. Langey, “Magnetorheologic fluids for actuators, Sensors and Actuators”, vol. 92, no. 1, pp. 318-325 2001. CrossRef

[4] M. M. Rashid, N. A. Rahim, M. A. Hussain, and M. Rahman, "Analysis and experimental study of magnetorheological-based damper for semiactive suspension system using fuzzy hybrids," IEEE Transactions on Industry Applications, vol. 47, pp. 1051-1059, 2011. CrossRef

[5] G. Yang, B. Spencer Jr, J. Carlson, and M. Sain, “Large-scale MR fluid dampers: modeling and dynamic performance considerations”, Engineering structures, vol. 24, no.3, pp. 309-323, 2002. CrossRef

[6] B. F. Spencer Jr, G. Yang, J. D. Carlson, and M. K. Sain, "Smart dampers for seismic protection of structures: a full-scale study," in Proceedings of the second world conference on structural control, 1998, pp. 417-426.

[7] Y.-T. Choi and N. M. Wereley, “Self-Powered Magnetorheological Dampers”, Journal of Vibration and Acoustics, vol. 131, no. 4, p. 044501, 2009. CrossRef

[8] Y.D. Liu, B. J. Park, F. F. Fang, H. J. Choi, and W.-S. Ahn, “Ironoxide/MCM-41 mesoporous nanocomposites and their magnetorheology”, Colloid and Polymer Science, Mar. 2013.

[9] H. H. Sim, S. H. Kwon, and H. J. Choi, “Xanthan gum-coated soft magnetic carbonyl iron composite particles and their magnetorheology”, Colloid and Polymer Science, vol. 291, no. 4, pp. 963–969, Sep. 2012. CrossRef

[10] L. A. Powell, N. M. Wereley, and J. Ulicny, "Magnetorheological fluids employing substitution of nonmagnetic for magnetic particles to increase yield stress," IEEE Transactions on Magnetics,, vol. 48, pp. 3764-3767, 2012. CrossRef

[11] Ferdaus, Mohammad Meftahul, et al. “Novel design of a self-powered and self-sensing magneto-rheological damper”, IOP Conference Series: Materials Science and Engineering. Vol. 53. No. 1. IOP Publishing, 2013.

[12] C. Chen and W.-H. Liao, “A self-sensing magnetorheological damper with power generation”, Smart Materials and Structures, vol. 21, no. 2, p. 025014, Feb. 2012. CrossRef

[13] M. M. Ferdaus, M. M. Rashid, M. H. Hasan, and M. A. Rahman, "Optimal design of Magneto-Rheological damper comparing different configurations by finite element analysis," Journal of mechanical science and technology, vol. 28, pp. 3667-3677, 2014.

[14] H. H. Zhang, “A Magnetic Design Method of MR Fluid Dampers and FEM Analysis on Magnetic Saturation”, Journal of Intelligent Material Systems and Structures, 17 (8-9) (2006) 813–818. CrossRef

[15] Z. Parlak, T. Engin, and İ. Çallı, “Optimal design of MR damper via finite element analyses of fluid dynamic and magnetic field”, Mechatronics, vol. 22, no. 6, pp. 890–903, Sep. 2012. CrossRef